On the use of simulated annealing to automatically assign decorrelated components in second-order blind source separation

Article *in* IEEE Transactions on Biomedical Engineering · June 2006

DOI: 10.1109/TBME.2005.863968 · Source: OAI

CITATIONS
6

READS
68

9 authors, including:

Peter Gruber
RevenuPath Deutschland GmbH
42 PUBLICATIONS **325** CITATIONS
SEE PROFILE

Fabian J Theis
Helmholtz Zentrum München
862 PUBLICATIONS **16,698** CITATIONS
SEE PROFILE

Elmar Wolfgang Lang
Universität Regensburg
279 PUBLICATIONS **2,482** CITATIONS
SEE PROFILE

Ana Maria Tomé
University of Aveiro
211 PUBLICATIONS **1,415** CITATIONS
SEE PROFILE

On the Use of Simulated Annealing to Automatically Assign Decorrelated Components in Second-Order Blind Source Separation

M. Böhm, K. Stadlthanner, P. Gruber, F. J. Theis, *Member, IEEE*, E. W. Lang*, A. M. Tomé, *Member, IEEE*, A. R. Teixeira, W. Gronwald, and H. R. Kalbitzer

***Abstract*—In this paper, an automatic assignment tool, called BSS-AutoAssign, for artifact-related decorrelated components within a second-order blind source separation (BSS) is presented. The latter is based on the recently proposed algorithm dAMUSE, which provides an elegant solution to both the BSS and the denoising problem simultaneously. BSS-AutoAssign uses a local principal component analysis (PCA)to approximate the artifact signal and defines a suitable cost function which is optimized using simulated annealing. The algorithms dAMUSE plus BSS-AutoAssign are illustrated by applying them to the separation of water artifacts from two-dimensional nuclear overhauser enhancement (2-D NOESY) spectroscopy signals of proteins dissolved in water.**

***Index Terms*—Blind source separation, generalized eigenvalue decomposition, matrix pencil, simulated annealing, 2-D NOESY NMR.**

I. Introduction

BLIND SOURCE separation (BSS) methods consider the separation of observed sensor signals into their underlying source signals knowing neither these source signals nor the mixing process. Considering biomedical applications, BSS methods are especially valuable to remove artifacts from the signals recorded. With noisy signals, this artifact removal, however, inevitably increases the noise level in the reconstructed, artifact-free signals. Hence, denoising techniques need to be considered to reduce the noise level of the reconstructed signals to the level of the original signals, at least.

In many biomedical applications, quite a number of underlying components have to be determined with BSS algorithms and it is not *a priori* clear how many components should be assigned to the signals representing the artifacts. Especially the signal of the physiological solvent, H_2O, is by far the most intense feature in ^1H nuclear magnetic resonance (NMR) spectroscopy of biological macromolecules and causes spectral artifacts even where strongly attenuated by presaturation or selective excitation. This is for example obvious in 2-D NOESY NMR proton spectra of proteins [1], where the prominent water artifact distorts the recorded spectra considerably. Many efforts have been undertaken to remove it. However, most of them have only been partially successful so far with the recovery of protein signals buried under the water artifact being one of the most difficult problems. Since as a consequence of the often used presaturation of the water resonance, the water signal is strongly phase distorted in the various component spectra belonging to deliberately incremented evolution periods within the pulse sequence. This, however, prohibits any simple analytical or wavelet-based fitting of the water artifact and subsequent subtraction from the recorded spectrum without loss of buried protein signals.

As experimental means seem unable to suppress the artifact sufficiently, only computational signal processing techniques may be able to solve the problem satisfactorily. In the following, some of the methods published so far for solvent suppression will be summarized.

The dispersive tails of the water resonance can be mainly removed from spectra by fitting these tails to a hyperbolic function which is then removed from the data [2]. A somewhat simpler method, similar to the diagonal peak suppression method for phase-sensitive COSY spectra, [3] makes use of the fact that the water resonance is usually positioned at the center of the spectrum (i.e., at $\omega = 0$). As a consequence, its time domain signal can be described as a nonmodulated exponential. The contribution of the water signal can be obtained by filtering out the oscillatory parts of the free induction decays (FIDs) and then subtracting those parts from the original time domain data [4]. The dispersive tails of the water resonance can also be suppressed by phasing the water signal in absorption mode, zeroing the relatively small absorption signal in the frequency domain data, discarding the imaginary part and regenerating the signal from the processed real part via a Hilbert transformation [5]. Also, it is possible to compute the second derivatives of the FIDs and to Fourier transform the latter, which also suppresses signals at $\omega = 0$, such as the water artifact [6]. Application of the Karhunen-Loeve transformation to multidimensional data removes undesired water artifacts based on their large intensity [7]. Similar results can be obtained by a principal component analysis of the frequency domain data [8] or linear prediction of the time domain data and removal of very strong singular values (signals) [9]. Also wavelet transformation can be used for solvent suppression. Here the signal is decomposed in terms of elementary contributions called wavelets. By discarding compo-

Manuscript received December 17, 2004; revised September 11, 2005. This work was supported in part by the DFG (graduate college 638), in part by the BMBF under Project ModKog, in part by the DAAD, and in part by the CRUP (Acção Integrada-Luso-Alemã). *Asterisk indicates corresponding author.*

M. Böhm, K. Stadlthanner, P. Gruber, and F. J. Theis are with the Institute of Biophysics, AG Neuro- and Bioinformatics, University of Regensburg, D-93040 Regensburg, Germany.

*E. W. Lang is with the Institute of Biophysics, AG Neuro- and Bioinformatics, University of Regensburg, D-93040 Regensburg, Germany (e-mail: elmar.lang@biologie.uni-regensburg.de).

A. M. Tomé and A. R. Teixeira are with the DETUA/IEETA, Universidade de Aveiro, P-3810-193 Aveiro, Portugal (e-mail: ana@ieeta.pt).

W. Gronwald and H. R. Kalbitzer are with the Institute of Biophysics, University of Regensburg, D-93040 Regensburg, Germany.

Digital Object Identifier 10.1109/TBME.2005.863968

nents corresponding to low frequencies before data reconstruction the water signal can be suppressed (assuming that the water is located in the middle of the spectrum) [10]–[12].

Recently artifact removal was considered using BSS techniques based on a generalized eigenvalue decomposition (GEVD) of a matrix pencil which is computed considering second-order statistics only [13], [14]. The method is very efficient and fast and outperformed FastICA and SOBI in all cases studied [15]. But, the estimated components related with the water artifacts had to be assigned by hand. With more than 100 estimated components this turns out to become a rather tedious undertaking prone to be biased by subjective judgements of the assignment criteria.

In this paper, we propose to use local principal component analysis (PCA) to approximate the FID related with the water artifact and to use simulated annealing (SA) [16] to identify those underlying uncorrelated components which were estimated with a GEVD using matrix pencils and which have to be assigned to the water artifact. Nullifying these components, an artifact-free protein spectrum can be reconstructed albeit at the expense of an increased noise level. Replacing the GEVD with the algorithm dAMUSE [17], BSS and denoising can be achieved simultaneously.

The algorithm dAMUSE considers an embedding of the noisy signal in a high-dimensional feature space of delayed coordinates [18]. The technique is similar to singular spectral analysis (SSA) [19] where trajectory matrices formed with delayed versions of a signal are subject to a singular value decomposition to extract informative components underlying the recorded signals. De-noising can be achieved by back-projecting the data into a lower dimensional subspace corresponding to the dimension of the underlying source signals. The algorithm dAMUSE, a modified version of AMUSE [20], comprises a simultaneous diagonalization of a matrix pencil whereby the latter is formed with correlation matrices computed in a high-dimensional feature space, i.e., after increasing the data set dimension by joining delayed versions of each sensor signal. dAMUSE, thus, solves the BSS problem, albeit a filtering indeterminacy remains, and simultaneously provides an efficient denoising tool.

The following section will provide a short summary of the algorithm dAMUSE [21], encompassing the matrix pencil algorithm (GEVD-MP) [13], and introduces the new algorithm BSS-AutoAssign. To illustrate the proposed method, some applications are discussed comprising theoretical 2-D NOESY NMR spectra with added noise and an experimental water resonance added as well. Further water artifacts have been removed from experimental 2-D NOESY protein spectra.

II. Theory

A. BSS Model

Given N complex sensor signals $x(t_{1,n}, t_{2,l}) \equiv x_n[l]$ sampled at L discrete time instances, the corresponding data matrix $\mathbf{X}$ reads

$$\mathbf{X} = \begin{bmatrix} x_1[0] & x_1[1] & \dots & x_1[L-1] \\ x_2[0] & x_2[1] & \dots & x_2[L-1] \\ \vdots & \vdots & \ddots & \vdots \\ x_N[0] & x_N[1] & \dots & x_N[L-1] \end{bmatrix} \tag{1}$$

where the rows of the data matrix correspond to one-dimensional (1-D) FIDs of the 2-D NOESY experiment taken at N discrete evolution times $t_{1,n} \equiv [n]$, $n = 1, \dots, N$.

BSS then relies on the following linear mixing model ($l = 0, \dots, L-1$)

$$\mathbf{x}[l] = \mathbf{A}\mathbf{s}[l] + \boldsymbol{\epsilon}[l] \tag{2}$$

where $\mathbf{x}[l] = (x_1[l], \dots, x_N[l])^T$ designates the observed signals sampled at time instance l, i.e., the lth column of the data matrix $\mathbf{X}$, $\mathbf{s}[l]$ the underlying uncorrelated source signals, $\mathbf{A}$ the stationary mixing matrix and $\boldsymbol{\epsilon}[l]$ an additional zero mean white Gaussian noise term. After Fourier transformation one obtains

$$\hat{\mathbf{x}}[\omega] = \mathbf{A}\hat{\mathbf{s}}[\omega] + \hat{\boldsymbol{\epsilon}}[\omega] \tag{3}$$

which shows that the linear mixing model holds in the frequency domain as well.

Considering 2-D NMR spectra, after Fourier transformation of the observed FIDs $x(t_{1,n}, t_{2,l}) \equiv x_n[l]$ with respect to the aquisition time $t_{2,l} \equiv [l]$ one obtains ($\hat{x}(t_{1,n}, \omega_{2,l}) \equiv \hat{x}_n[l]$)

$$\hat{\mathbf{x}}[l] = \sum_{n=1}^{N} \mathbf{a}_n \hat{s}_n[l] + \hat{\boldsymbol{\epsilon}}[l] \tag{4}$$

where $\hat{\mathbf{x}}[l]$ denotes the N-dimensional vector of spectral amplitudes at frequency $\omega_{2,l} \equiv [l]$ of the N 1-D spectra. The latter form the rows of the data matrix $\hat{\mathbf{X}}$ in frequency space, whereas the $\hat{\mathbf{x}}[l]$ form the corresponding columns. The N 1-D spectra correspond to N discrete evolution periods $t_{1,n} \equiv [n]$. The columns $[l]$ of the source signal matrix $\hat{\mathbf{S}}$ comprise the spectral contents at frequency $\omega_l \equiv [l]$ of the N underlying and uncorrelated 1-D spectra. Their contribution to the observed spectral amplitudes $\hat{\mathbf{x}}[l]$ is given by the mixing coefficients $\mathbf{a}_n$. Hence, a linear superposition model is appropriate to describe each 1-D NMR spectrum and the BSS model considered above can be applied to 2-D NOESY NMR spectra.

B. Embedding Signals in a Feature Space of Delayed Coordinates

A GEVD technique [20] using congruent matrix pencils (GEVD-MP) [13] may be used to separate the water artifact from 2-D NOESY NMR spectra of proteins as has been shown recently [22]. Later the GEVD-MP algorithm [23] has been extended to data embedded in a high-dimensional feature space of delayed coordinates, resulting in the algorithm dAMUSE [17], [21]. The latter provides a means to perform BSS and denoising in parallel [24]. The method uses the concept of a trajectory matrix borrowed from SSA (see [19] for a recent review).

Considering L samples and M delayed versions of a sensor signal component $x_n[l]$, each column of a component trajectory matrix $\mathbf{X}_n^e$ [25] contains delayed versions $x_n[l-mK]$, where K denotes the delay in number of sample points between consecutive rows, $l = (M-1)K, \dots, L-1$ and $m = 0, 1, \dots, M-1$. The resulting component trajectory matrix will have a Toeplitz structure with the same samples repeated along diagonals. The

total trajectory matrix $\mathbf{X}^e$ of N sensor signals is formed by concatenating the component trajectory matrices $\mathbf{X}_n^e$ according to

$$\mathbf{X}^e = [\mathbf{X}_1^e, \mathbf{X}_2^e, \ldots, \mathbf{X}_N^e]^T. \tag{5}$$

After embedding, the instantaneous mixing model can be written as $\mathbf{X}^e = \mathbf{A}^e\mathbf{S}^e$ where $\mathbf{S}^e$ represents the source signal trajectory matrix and $\mathbf{A}^e = \mathbf{A}_n \otimes \mathbf{I}_{M\times M}$ forms a block matrix with $\mathbf{I}_{M\times M}$ being the identity matrix. Then if $\mathbf{A}_n$ is an invertible matrix, $\mathbf{A}^e$ is also invertible as it is the Kronecker product of two invertible matrices.

Recently the algorithm dAMUSE [17], [24] was proposed to use such data embedded in a high-dimensional feature space to simultaneously solve the blind source separation problem and reduce the noise level of the reconstructed signals. dAMUSE proposed a two-step GEVD of a matrix pencil, whereby the corresponding correlation matrices of the pencil are computed with suitably chosen feature vectors. Here, in addition, an alternative way of computing one of the matrices of the pencil will be described in the following section and a brief review of the characteristics of the resulting solution will be given.

C. On the Use of a Filtering Operation to Compute the Pencil

Some second-order methods based on a GEVD perform a simultaneous diagonalization of a matrix pencil. However, the second correlation matrix of the pencil can be computed using different strategies [13], [23], [26]. Here we propose a filtering operation performed in the frequency domain while the correlation operation is performed in the time domain.

The discrete Fourier transform (1-D) of the embedded data is computed first. Next each entry in each row of the total trajectory matrix $\hat{\mathbf{X}}^e$ is multiplied by a corresponding element of a Gaussian filter function $\hat{h}[l]$. In matrix notation this yields $\hat{\mathbf{X}}_F^e = \hat{\mathbf{X}}^e \diamond \hat{\mathbf{H}}$ where $\diamond$ represents the Hadamard product and $\hat{\mathbf{H}}$ contains the samples $\hat{h}[l]$ in all rows.

Note that the discrete product operation in the frequency domain corresponds to a circular convolution in the time domain as can be shown easily. Given the inverse transform $h[l]$, $l = 0, \ldots, J-1$, $J \equiv L-(M-1)K$ of the bandpass filter frequency response function, the circular convolution for an arbitrary signal $\mathbf{c} = (c[0], \ldots, c[J-1])^T$ can be computed using a matrix manipulation $\mathbf{z} = \mathbf{H}\mathbf{c}$, as shown in (6) at the bottom of the page, where the matrix $\mathbf{H}$ is a circular matrix with circularly shifted columns of the impulse response $h[l]$. Computing the transpose of each member of (6) yields $\mathbf{z}^T = \mathbf{c}^T\mathbf{H}^T$, where the input and output signals are organized in rows. Applied to the sensor signals considered here, filtering each row of the trajectory matrix $\mathbf{X}^e$ will be achieved by $\mathbf{Z} = \mathbf{X}^e\mathbf{H}^T$, where each row of $\mathbf{Z}$ represents a filtered version of the corresponding row of $\mathbf{X}^e$. The correlation matrices computed with the original and the filtered data, respectively, then form the pencil $(\mathbf{R}_x, \mathbf{R}_{x,F})$ whereby

$$\begin{aligned}\mathbf{R}_x &= \left\langle \mathbf{X}^e(\mathbf{X}^e)^H \right\rangle \\ \mathbf{R}_{x,F} &= \langle \mathbf{Z}\mathbf{Z}^H \rangle = \left\langle \mathbf{X}^e(\mathbf{H}^H\mathbf{H})^T(\mathbf{X}^e)^H \right\rangle.\end{aligned} \tag{7}$$

Substituting $\mathbf{X}^e = \mathbf{A}^e\mathbf{S}^e$, this pair of correlation matrices forms a congruent pencil with an equivalent pair of matrices computed in the source domain. A GEVD with simultaneous denoising of the given matrix pencil can then be achieved applying the algorithm dAMUSE as has been explained elsewhere [17]. Hence, we only summarize some characteristics of the solutions obtained.

The eigenvector matrices of the sensor pencil and source pencil, respectively $\mathbf{E}_x$ and $\mathbf{E}_s$, are related by the mixing matrix $\mathbf{A}^e$ via $\mathbf{E}_s = (\mathbf{A}^e)^H\mathbf{E}_x$ [17]. Furthermore, $\mathbf{E}_x$ provides a solution to the BSS problem if the source signals are uncorrelated as the following holds:

- With nonembedded signals ($K = 1$ and $M = 1$, hence, $\mathbf{A}^e = \mathbf{A}$) the eigenvector matrix $\mathbf{E}_s$ corresponds to the identity matrix and the Hermitian conjugate of the eigenvector matrix of the sensor pencil $\mathbf{E}_x^H$ forms an estimate of the separation matrix [13]. In that case, $\mathbf{Y} = \mathbf{E}_x^H\mathbf{X}$ yields an estimate of the source signals.
- With embedded signals, the GEVD of the matrix pencil $(\mathbf{R}_x, \mathbf{R}_{x,F})$ will provide the linear transformation to be applied to the embedded data, i.e., $\mathbf{Y} = \mathbf{E}_x^H\mathbf{X}^e$. Hence, the transformed trajectory matrices then read

$$\mathbf{Y} = \mathbf{E}_x^H\mathbf{X}^e = \mathbf{E}_x^H\mathbf{A}^e\mathbf{S}^e = \mathbf{E}_s^H\mathbf{S}^e. \tag{8}$$

  Assuming that the source signals and their filtered versions are uncorrelated, the matrix $\mathbf{E}_s$ is block-diagonal, with block size $(M \times M)$. Thus, each entry of $\mathbf{Y}$ is a weighted sum of a source signal and its delayed versions [24].

If the GEVD of the matrix pencil $(\mathbf{R}_x, \mathbf{R}_{x,F})$, i.e., the computation of the separation matrix $\mathbf{E}_x^H$, is implemented using a two step strategy, then a simultaneous denoising of the extracted signals can be achieved as has been explained elsewhere [17]. Note that in this case the number of output signals $\mathbf{Y}$ will be smaller than the one of the embedded input signals $\mathbf{X}^e$ (NM signals). We consider the two-step implementation with concomitant denoising in the results section where it will be referred to as the dAMUSE algorithm.

D. The Algorithm BSS-AutoAssign

The proposed algorithm is applicable to blind source separation algorithms in general. It is demonstrated here for second-order BSS. The method may apply equally to independent component analysis (ICA) which exploits higher order statistics. Its

$$\begin{bmatrix} z[0] \\ z[1] \\ z[2] \\ \vdots \\ z[J-1] \end{bmatrix} = \begin{bmatrix} h[0] & h[J-1] & h[J-2] & \cdots & h[1] \\ h[1] & h[0] & h[J-1] & \cdots & h[2] \\ h[2] & h[1] & h[0] & \cdots & h[3] \\ \vdots & \vdots & \vdots & \ddots & \vdots \\ h[J-1] & h[J-2] & h[J-3] & \cdots & h[0] \end{bmatrix} \begin{bmatrix} c[0] \\ c[1] \\ c[2] \\ \vdots \\ c[J-1] \end{bmatrix} \tag{6}$$

essential ingredients to the cost function defined below are uncorrelated (or independent) components of the signals recorded. The way these components have been estimated is of no importance to the performance of the algorithm. The current discussion is based on second-order techniques using additional information about time correlations of the recorded signals. This is done deliberately so as the much stronger assumption of statistically independent source signals is hard to justify in case of NMR signals.

Applying the BSS algorithms discussed above to 2-D NOESY NMR spectra to separate the water artifact and related artifacts from the protein spectra, the most tedious task is to assign the uncorrelated components estimated to the water signal. Because of erratic phase relations, up to 160 estimated components out of 512 need to be assigned to the water resonance. Hence, an automated and objective assignment procedure is deemed necessary.

In a first series of steps, data will be embedded in a feature space of delayed coordinates, clustered according to an Euclidian similarity measure and then the embedded and clustered data are decomposed into their principal components.

1) Embedding and Local PCA: Embedding signals in a high-dimensional feature space of time-delayed coordinates represents a nonlinear operation which can be approximated by a piecewise linear operation performing PCA locally on clusters of similar feature vectors. Retaining only the component belonging to the largest eigenvalue extracts the dominant linear feature locally in each cluster. These locally dominant features are then combined to approximate the dominant global feature in the data which has to be related to the water artifact.

1) Consider a signal

$$\mathbf{x}_n[l] = (x_n[l], x_n[l+1], \ldots, x_n[l+(M-1)])^T \quad (9)$$

embedded in an M-dimensional feature space. This multidimensional signal represents one out of $(L-(M-1))$ columns of the related component trajectory matrix considering $K=1$ (see Section II-B).

2) Divide the feature space in k_c subsets $\mathcal{N}^{(i)}$, $i=1,\ldots,k_c$ using k-*means* clustering of the embedded signal vectors $\mathbf{x}_n[l]$ and center the signals in each cluster locally by subtracting the cluster mean given by

$$\left\langle \mathbf{x}_n^{(i)} \right\rangle = \left|\mathcal{N}^{(i)}\right|^{-1} \sum_{\mathbf{x}_n[l]\in\mathcal{N}^{(i)}} \mathbf{x}_n[l], \quad i=1,\ldots,k_c. \quad (10)$$

3) Next, a PCA is performed on each cluster separately, and a *local* approximation to the time domain signal is computed using only the eigenvectors $\mathbf{p}_j^{(i)}$ corresponding to the $q(i)$ largest eigenvalues according to

$$\tilde{\mathbf{x}}_n[l] = \sum_{j=1}^{q(i)} \alpha_j[l]\mathbf{p}_j^{(i)} + \left\langle \mathbf{x}_n^{(i)} \right\rangle \quad (11)$$

with $\alpha_j[l] = \mathbf{x}_n[l]\cdot\mathbf{p}_j^{(i)}$ and $\mathbf{x}_n[l]\in\mathcal{N}^{(i)}$.

4) As the water signal provides the dominant contribution to each interferogram observed, the local PCA approximation can be simplified further by retaining only the principal component to the largest eigenvalue, i.e.

$$\tilde{\mathbf{x}}_n[l] = \alpha_1[l]\mathbf{p}_1^{(i)} + \left\langle \mathbf{x}_n^{(i)} \right\rangle. \quad (12)$$

This approximation to the observed FID supposedly contains the contribution from the water signal almost exclusively.

5) The clustering process is reverted then whereby each original column vector $\mathbf{x}_n[l]$ is replaced by its local PCA approximation $\tilde{\mathbf{x}}_n[l]$.

6) A new component trajectory matrix $\tilde{\mathbf{X}}_n$ is then formed, the entries of which represent local PCA approximations of the original signals

$$\tilde{\mathbf{X}}_n = \begin{bmatrix} \tilde{x}_n[M-1] & \tilde{x}_n[M] & \ldots & \tilde{x}_n[L-1] \\ \tilde{x}_n[M-2] & \tilde{x}_n[M-1] & \ldots & \tilde{x}_n[L-2] \\ \tilde{x}_n[M-3] & \tilde{x}_n[M-2] & \ldots & \tilde{x}_n[L-3] \\ \vdots & \vdots & \ddots & \vdots \\ \tilde{x}_n[0] & \tilde{x}_n[1] & \ldots & \tilde{x}_n\left[(L-1)-(M-1)\right] \end{bmatrix}. \quad (13)$$

7) The final global approximation $\langle \tilde{\mathbf{x}}_n[l]\rangle_{[l]}$, $l = M-1, \ldots, L-1$ of every feature vector then may be obtained by averaging all entries to the component trajectory matrix corresponding to the same time instance $[l]$. Due to the Toeplitz structure of the trajectory matrix these entries lie along diagonals.

The local PCA approximation of the feature vectors can now be compared with a weighted linear combination of estimates of uncorrelated components obtained with the algorithm dAMUSE. Note that the reconstructed signal, thus obtained, represents the water artifact overlaying the protein spectra. In the following, we will use SA [16] to filter out those uncorrelated components which are needed to represent the water artifact. The idea is that those components should most closely resemble the approximate feature vector obtained above.

2) Simulated Annealing: The local PCA approximation to the FID related with the water artifact deduced in Section II-D1 is then used to define a cost function

$$\mathcal{E}(\boldsymbol{\beta}) = \sum_{l=0}^{L-1} \left(x^e_{n,\boldsymbol{\beta}}[l] - \langle \tilde{x}_n[l]\rangle\right)^2 \quad (14)$$

to be minimized with SA [16]. The BSS approximation to the water signal using the uncorrelated components estimated as described in Section II-C is obtained as

$$x^e_{n,\boldsymbol{\beta}}[l] = \sum_j w_{nj}\beta_j y_j[l] \quad (15)$$

where a configuration is represented by a vector $\boldsymbol{\beta}$ which contains as many components β_j as there are filtered sources $\mathbf{y}_j$. Note, that it is sufficient to consider the filtered versions of the underlying source signals as the interest is only in the reconstruction of the "artifact-free" original signals. To every source one element of $\boldsymbol{\beta}$ is assigned which can take on the values $\beta_j \in \{0,1\}$ only. A new configuration $\boldsymbol{\beta}$ is generated by changing any $\beta_j \in \{0,1\}$ randomly. Each configuration, thus, consists

only of those sources, whose corresponding element in $\boldsymbol{\beta}$ exhibits the value 1. In addition, each source is weighted with the corresponding entry w_{nj} of the mixing matrix $\mathbf{W} = (\mathbf{E}_x^H)^\dagger$ of the filtered sources $\mathbf{Y}$ [see (8)] using the Moore—Penrose pseudo-inverse of the eigenvector matrix $\mathbf{E}_x^H$. The difference in the values of the cost function for the current and the new configuration

$$\Delta\mathcal{E} = \mathcal{E}(\boldsymbol{\beta}_{\text{new}}) - \mathcal{E}(\boldsymbol{\beta}_{\text{old}}) \tag{16}$$

determines the probability of acceptance of the new configuration in the SA algorithm using Metropolis sampling [16] according to

$$P[\boldsymbol{\beta}_{\text{old}} \rightarrow \boldsymbol{\beta}_{\text{new}}] = \min\left\{1, \exp\left(-\frac{\Delta\mathcal{E}}{k_B T}\right)\right\}. \tag{17}$$

After convergence of the SA algorithm, the configuration which best fits to the local PCA approximation of the water signal is obtained.

E. Signal Reconstruction

In order to obtain the reconstructed signal the following steps are made.

- Apply dAMUSE (or any other BSS-algorithm) to the sensor signals $\mathbf{X}$ to extract the underlying uncorrelated components
- Approximate the water signal contained in the first sensor signal $\mathbf{x}_1$ corresponding to the shortest evolution period with a local PCA estimate
- Identify with SA those uncorrelated components, which make a contribution to the water signal; as cost function the quadratic error of the local PCA approximation to the water signal minus a weighted linear superposition of uncorrelated components is taken in order to obtain the combination of those uncorrelated components which best corresponds to the local PCA approximation of the water signal
- Nullify those uncorrelated components which contribute to the water artifact: $\mathbf{y}_n \rightarrow \mathbf{y}_n^\dagger$
- Reconstruct the trajectory matrix $\mathbf{X}^e$ using the estimated source signals $\mathbf{y}_n^\dagger$ via $\mathbf{X}^e = (\mathbf{E}_x^H)^\dagger \mathbf{Y}^\dagger$
- The original sensor signals (interferograms) can be extracted from the reconstructed trajectory matrix $\mathbf{X}^e$ by simply selecting the nondelayed signal vectors contained in the rows of the matrix.

The water signal contributing to the complex interferogram observed exhibits a similar shape for all evolution periods, it is assumed that the water signal in every interferogram is generated by contributions from the same uncorrelated components. The respective weight of the contributions is determined by the mixing matrix. Hence, it is sufficient to identify those uncorrelated components, which contribute to the water signal, for one interferogram only, namely the one corresponding to the shortest evolution period. This speeds up the computation considerably, because the optimization has to be applied only once and not as many times as there are different interferograms corresponding to different evolution periods.

III. Results and Discussion

The algorithms discussed above have been applied to artificial as well as experimental 2-D NOESY proton NMR spectra of proteins dissolved in water. Experimentally, a simple pre-saturation of the water resonance was applied to prevent saturation of the dynamic range of the analog-digital-converter. Every data set comprises 512 or 1024 FIDs $S(t_1, t_2) \equiv x_n[l]$ or their corresponding spectra $\hat{S}(t_1, \omega_2) \equiv \hat{x}_n[l]$, with $L = 2048$ samples each, which correspond to $N = 128$ or $N = 256$ FIDs evaluated at $t_1 \equiv [n]$. With each increment of the evolution period also the phase is incremented, hence, only FIDs with equal phase modulations have been grouped together for analysis. A BSS analysis, using the algorithm dAMUSE in combination with BSS-AutoAssign, was applied to all data sets. Note that in the algorithm dAMUSE, in spite of the filtering operation being performed in the frequency domain, the matrix pencil was computed in the time domain as described in Section II-C. The GEVD is performed in dAMUSE as described in [21] to achieve a dimension reduction and concomitant denoising. The automatic assignment of the uncorrelated components belonging to the water resonance, which were estimated with the dAMUSE algorithm, was achieved using the proposed algorithm BSS-AutoAssign. To contrast the denoising capacity of the algorithm dAMUSE to the BSS algorithm GEVD-MP used in earlier studies [23], for the convenience of the reader, we include the results obtained with the latter in the tables given.

A. Artificial Spectra

For test purposes, a theoretical 2-D NOESY proton NMR spectrum of the cold-shock protein of the bacterium *Thermatoga maritima*, containing only protein resonances, was used. The spectrum was obtained through Fourier transformation of the first FID calculated with the algorithm RELAX [27] and is shown in [Fig. 1(a)]. Gaussian white noise with realistic amplitude as well as an experimentally recorded water resonance were added to the theoretical spectrum [see Fig. 1(b), (c)].

The BSS was done either with the GEVD-MP algorithm [23] or with the algorithm dAMUSE [24]. The second correlation matrix $\mathbf{R}_{x,F}$ of the pencil was computed with the theoretical spectrum with added noise taken as the filtered version of the original spectrum. An approximation of the water artifact dominating the time domain FIDs was obtained with the local PCA algorithm. As the experimental pure water FID was available also, both could be compared to access the quality of the approximation. To perform local PCA, each sample of the data was embedded in a $M = 40$ dimensional feature space and *k-means* clustering was used to divide the projected data into $k_c = 2$ clusters. Only the largest principal component was considered to reconstruct the data in each cluster as described in Section II-E. The local PCA approximation has been determined only for the shortest evolution period and it was assumed that the *assignment* of the artifact related sources estimated with the algorithm BSS-AutoAssign remained unchanged also for all other evolution periods.

Fig. Fig. 2(a) compares the total FID corresponding to the shortest evolution period with the FID of the experimental water signal [Fig. 2(b)] and the local PCA approximation [Fig. 2(c)] of the latter. It is immediately obvious that the water artifact

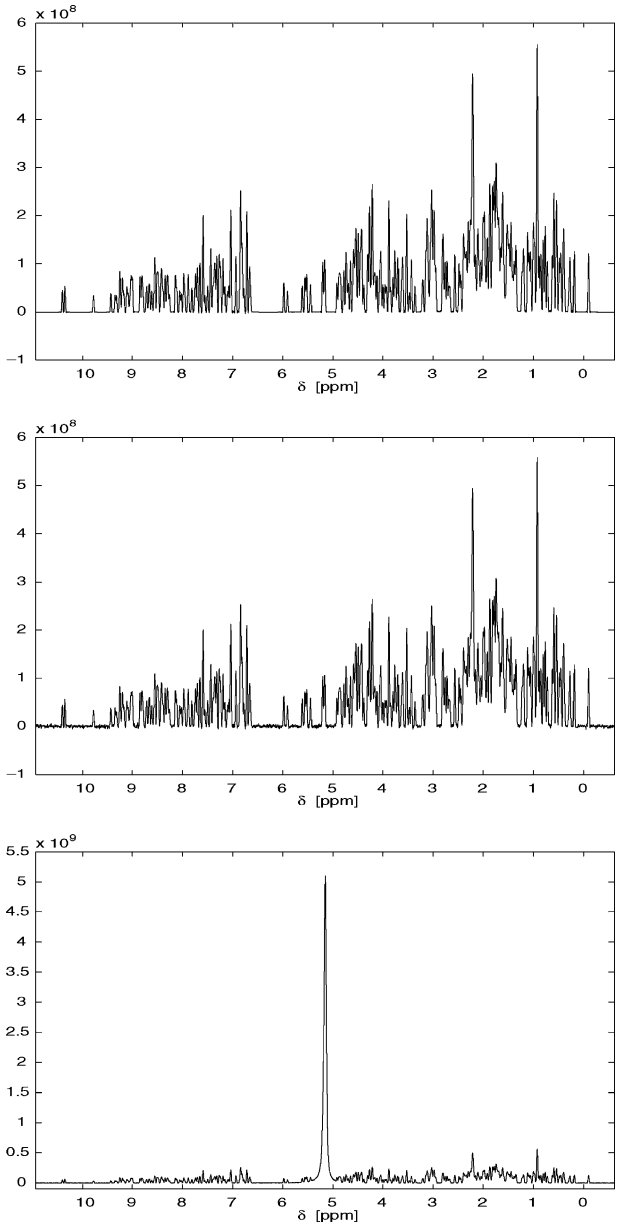

Fig. 1. *top*: Theoretical protein spectrum, *middle*: Theoretical protein spectrum with Gaussian noise, *bottom*: Theoretical spectrum with Gaussian noise and an experimental water resonance recorded without suppression.

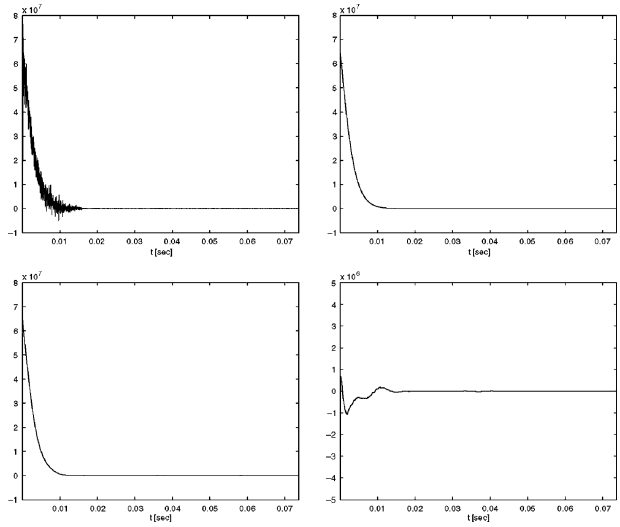

Fig. 2 Free Induction Decays (FID) of *top left*: the total FID of the protein signal plus additive noise plus the experimental water FID, *top right*: experimental FID of the water signal, *bottom left*: local PCA approximation of the total FID, *bottom right*: difference between the total FID and its local PCA approximation.

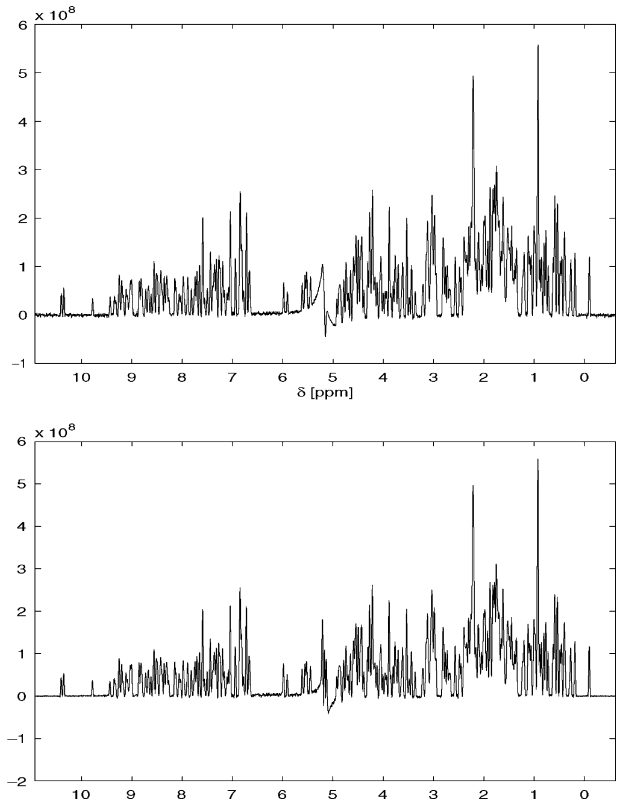

Fig. 3. *top*: Protein spectrum obtained after subtracting the approximated water FID from the total FID and Fourier transformation of the difference FID, *bottom*: Reconstructed protein spectrum obtained with the algorithm dAMUSE plus BSS-AutoAssign.

dominates the total FID. Finally, Fig. 2(d) gives the difference between the experimental FID and its local PCA approximation. It is seen that local PCA provides a very good approximation to the water artifact. This can be corroborated by subtracting the approximate water FID from the total FID and transforming the resulting FID into the frequency domain. The resulting protein spectrum contains only small remnants of the huge water artifact as can be seen in Fig. 3. The spectra, thus obtained, will henceforth be called *approximated spectra*.

This indicates that it should be possible to use the local PCA approximation of the water artifact as a reference signal in a cost function to be minimized with a SA algorithm. This is confirmed by analyzing the theoretical protein spectra plus noise plus water artifact [see Fig. 1(c)] with the GEVD-MP algorithm [23] to extract the uncorrelated components and using SA to automatically assign those components related with the water artifact. The SA-algorithm identifies the same 9 components irrespective whether the experimental water FID or its local PCA approximation has been used in the cost function.

The reconstructed protein spectrum [see Fig. 3(b)] (spectra obtained this way will henceforth be called *reconstructed*

TABLE I
SNRs OF THE ORIGINAL THEORETICAL SPECTRUM PLUS NOISE AND THE SPECTRA RECONSTRUCTED WITH EITHER GEVD-MP OR DAMUSE AND BSS-AUTOASSIGN

	SNR [dB]
orig. spectrum plus noise (Fig. 1-b))	24.5 dB
approximated spectrum (Fig. 3-a))	24.3 dB
GEVD-MP (Fig. 3-b))	10.1 dB
dAMUSE (Fig. 3-c))	22.1 dB

spectra) resembles the original noisy spectrum [Fig. 1(b)] except for a much enhanced noise level. Calculating the signal-to-noise ratio (SNR) via

$$\mathrm{SNR}(\mathbf{x}, \mathbf{x}_{\mathrm{noise}})[dB] = 20 \log_{10} \frac{\|\mathbf{x}\|}{\|\mathbf{x} - \mathbf{x}_{\mathrm{noise}}\|} \qquad (18)$$

where $\mathbf{x}$ denotes the theoretical spectrum, $\mathbf{x}_{\mathrm{noise}}$ its noisy counterpart, the theoretical spectrum plus gaussian noise shows a SNR of 24.5 dB, whereas the reconstructed protein spectrum obtained with the GEVD-MP algorithm only yields a SNR of 10.1 dB.

It, thus, appears, that the GEVD-MP procedure yields reconstructed spectra with an enhanced noise level due to the removal of part of the self-compensatory noise components together with the water related components. Hence, denoising is necessary as a post-processing to the reconstructed spectra obtained with the GEVD-MP algorithm.

But denoising can be accomplished elegantly with the dAMUSE algorithm [21] which achieves blind source separation and denoising simultaneously. The water related components extracted are automatically assigned with the algorithm BSS-AutoAssign using a local PCA approximation to the water artifact. The optimal dimension M of the feature space as well as the optimal time lag have been determined by the best minimum of the cost function obtained with the SA algorithm. A minimum of the cost function has been obtained with using a subspace dimension $M = 2$ in the trajectory matrix, a lag of one sampling interval $(K = 1)$ and by retaining 158 eigenvectors (out of $2 \cdot 128$) after the first step of the algorithm dAMUSE. The result of the dAMUSE denoising is shown in Fig. 3(c). The corresponding SNRs are collected in Table I.

The superior performance of the algorithm dAMUSE in combination with the algorithm BSS-AutoAssign is demonstrated by the fact that even protein resonances hidden behind the water artifact could be recovered this way. A close inspection of the results obtained with the theoretical spectra of *Tm*CSP demonstrate convincingly that dAMUSE plus BSS-AutoAssign retain information about spectral features in the region of the water artifact where the local PCA approximation and all other known water suppression techniques erase all spectral features whatsoever. This is clearly visible in Fig. 7 in the region between 5 ppm and 5.5 ppm where a doublet is hidden under the water resonance which can be recovered by the algorithm dAMUSE in combination with BSS-AutoAssign, but not with the local PCA approximation. This demonstrates that with the method described here it is possible to obtain additional structurally relevant restraints from the experimental NOESY spectra which will enter the structure calculation process. Furthermore, it can

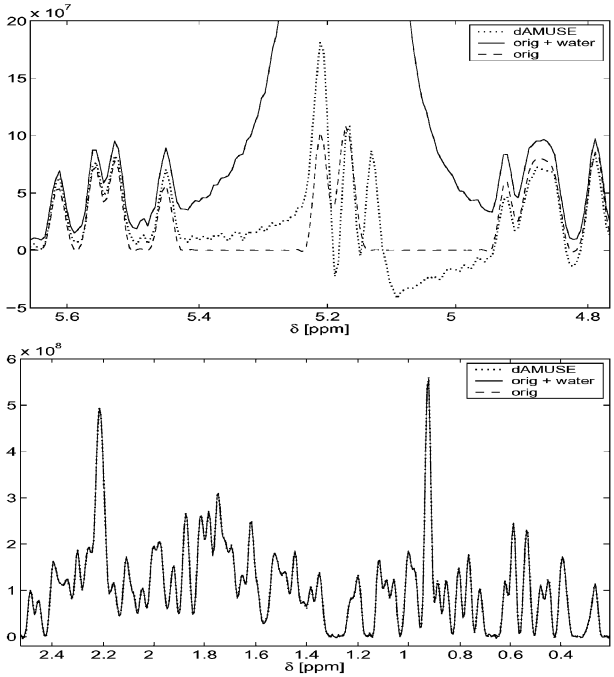

Fig. 4. *top*: Comparison of part of the theoretical (named orig.) TmCSP spectrum, the theoretical spectrum with an added experimental water resonance and the spectrum reconstructed with dAMSUE plus BSS-AutoAssign in the spectral region of the water peak. *bottom*: A similar comparison in a spectral region away from the water peak.

be seen from Fig. 4(a) that the baseline distortions are much reduced with the algorithms dAMUSE plus BSS-AutoAssign and also that the protein peaks are not distorted at all in the reconstructed spectrum as is shown in Fig. 4(b). This demonstrates the strength of the current algorithm to recover signals hidden behind the water artifact, to remove any baseline rolls stemming from the water artifact but leave any protein signals away from the water artifact undistorted. These features provide additional and improved distance constraints as well as better defined peak integrals entering a three-dimensional (3-D) structure determination.

B. Experimental Spectra

To test the performance of the algorithm BSS-AutoAssign in combination with the algorithm dAMUSE we applied it to four sets of 2-D NOESY proton NMR spectra of proteins dissolved in water. In each case, a number N_{IC} of uncorrelated components has been estimated using either the algorithm GEVD-MP or dAMUSE. Though results will be tabulated for all four protein solutions, only *Tm*CSP and HPr will be discussed here. For details concerning the proteins RALGDS and P11 see [17] and [23], respectively.

To get a local PCA approximation of the water artifact, data have been projected into a M_{localPCA}-dimensional feature space and k_c clusters have been determined in feature space with a *k-means* algorithm. Also a Gaussian filter with width σ centered near the water resonance in the 1-D proton NMR spectra has been used. The algorithm BSS-AutoAssign automatically identified a number N_w of uncorrelated components which have to be assigned to the water artifact with either the GEVD-MP or the dAMUSE algorithm being used to solve

TABLE II
PARAMETER VALUES FOR THE EMBEDDING DIMENSION OF THE FEATURE SPACE OF DAMUSE (M_{dAMUSE}) AND LOCALPCA (M_{localPCA}), THE NUMBER (K) OF SAMPLING INTERVALS USED PER DELAY IN THE TRAJECTORY MATRIX, THE NUMBER OF CLUSTERS (k_c) USED WITH LOCAL PCA IN BSS-AUTOASSIGN, THE NUMBER (N_{pc}) OF PRINCIPAL COMPONENTS RETAINED AFTER THE FIRST STEP OF THE GEVD [23] AND THE HALF-WIDTH (σ) OF THE GAUSSIAN FILTER USED IN THE ALGORITHMS GEVD-MP [23] AND DAMUSE

Parameter	TmCSP	RalGDS	P11	HPr
N_{IC}	256	256	256	512
$M_{localPCA}$	40	50	30	50
M_{dAMUSE}	2	4	3	2
k_c	2	2	2	2
N_{pc}	168	168	148	396
$N_w(GEVD)$	46	14	49	28
$N_w(dAMUSE)$	46	56	46	160
σ	0.3	0.1	0.3	0.03
K	1	1	1	1

TABLE III
SNRS OF THE RECONSTRUCTED SPECTRA OF TMCSP, RALGDS, P11 AND HPR OBTAINED WITH GEVD-MP [23] OR DAMUSE AND BSS-AUTOASSIGN

	SNR [dB]			
	TmCSP	RalGDS	P11	HPr
GEVD-MP	11.5	16.6	18.6	11.3
dAMUSE	19.3	21.9	21.9	19.8

the BSS problem. Remember that it is assumed that this assignment also holds for all other evolution periods as well. Note that all parameters have been varied systematically, and optimal parameters have again been selected according to the best minimum of the cost function of the SA-algorithm. These optimal parameters are collected in Table II.

With all experimental spectra the SNR has been determined relative to the *approximated* protein spectra, which were obtained by subtracting a local PCA approximation of the FID of the water artifact from the total FID as explained in the theory section. Hence, with all experimental spectra the corresponding *approximated* spectra formed the reference against which the *reconstructed* spectra have been compared. The SNRs of the reconstructed spectra obtained with either GEVD-MP (see [23] for details) or dAMUSE are summarized in Table III.

1) The Protein TmCSP: First we applied the algorithms to 2-D NOESY proton NMR spectra of the cold-shock protein *Tm*CSP of the bacterium *Thermatoga maritima*. It represents a small globular protein with 66 amino acids [28]. The experimental spectra analyzed were recorded from a sample of 1.5 mM cold shock protein in $92\%\mathrm{H_2O}/8\%\,\mathrm{D_2O}\,(v/v)$, pH 6.5. The spectrum using a mixing time of 160 ms was acquired at a proton resonance frequency of 800.13 MHz with 512×4096 time domain data points in t_1 and t_2 directions, respectively. Phase-sensitive detection in the t_1 direction was obtained using time-proportional phase increments (TPPI). A relaxation delay of 1.31 s between the scans was used and the temperature was adjusted to 303 K. These experimental spectra represent the counterpart to the theoretical spectra just discussed. A 1-D slice of the original 2-D NOESY spectrum corresponding to the shortest evolution period t_1 as well as the *approximated* protein spectrum are shown in Fig. 5(a), (b), respectively. The *reconstructed* protein spectrum obtained with the algorithm dAMUSE is also shown in Fig. 5(c). The much better SNR in case of the algorithm dAMUSE compared to GEVD-MP (see [17]) corroborates the necessity for a denoising of the signals during or after the BSS.

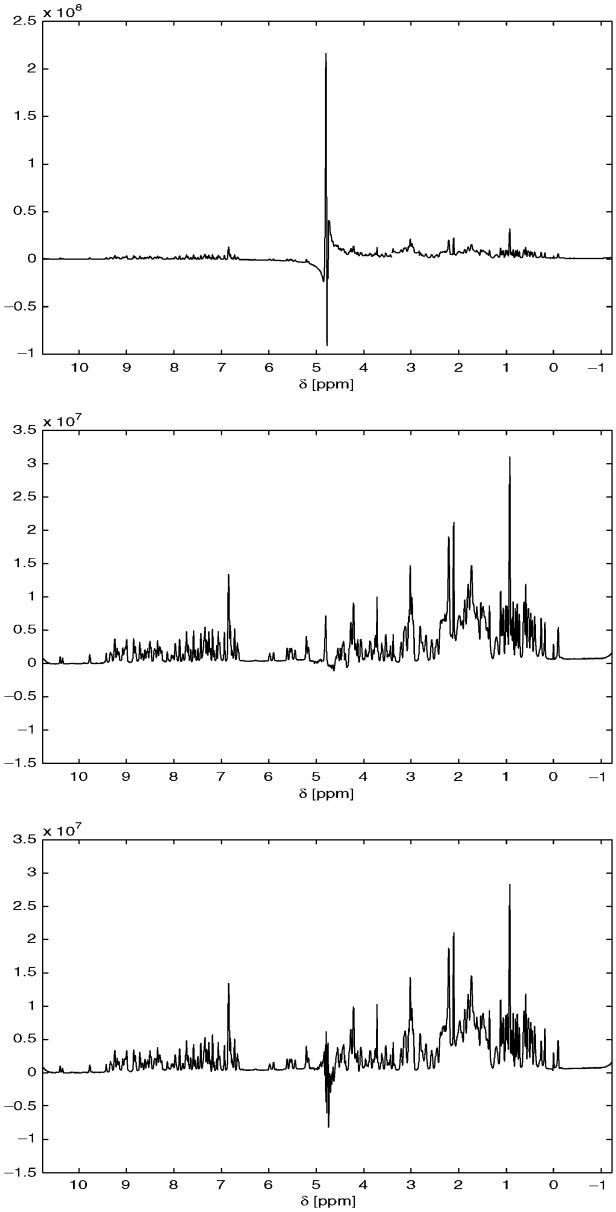

Fig. 5. *Tm*CSP: *top*: one-dimensional slice of the original 2-D NOESY spectrum corresponding to the shortest evolution period t_1, *middle*: corresponding protein spectrum obtained by subtracting the local PCA approximation to the water artefact FID from the total FID, *bottom*: protein spectrum reconstructed with the dAMUSE and BSS-AutoAssign algorithms.

Much the same holds with all other experimental spectra investigated. Further it is to be noted that applying the GEVD-MP algorithm with BSS-AutoAssign changes the intensities of the protein peaks to some extent. With the algorithm dAMUSE, instead, the protein peaks remain rather unchanged which is important to a reliable determination of the peak integrals entering the structure determination calculation. However, some small remnants of the water artifact still remain in some reconstructed spectra. But the baseline distortions are perfectly straightened out and even peaks very close to or even hidden behind the water artifact are well recovered as shown in case of *Tm*CSP. Note that there exists no other technique to recover peaks hidden by the water artifact. Hence, the new algorithm provides additional constraints to an improved structure determination.

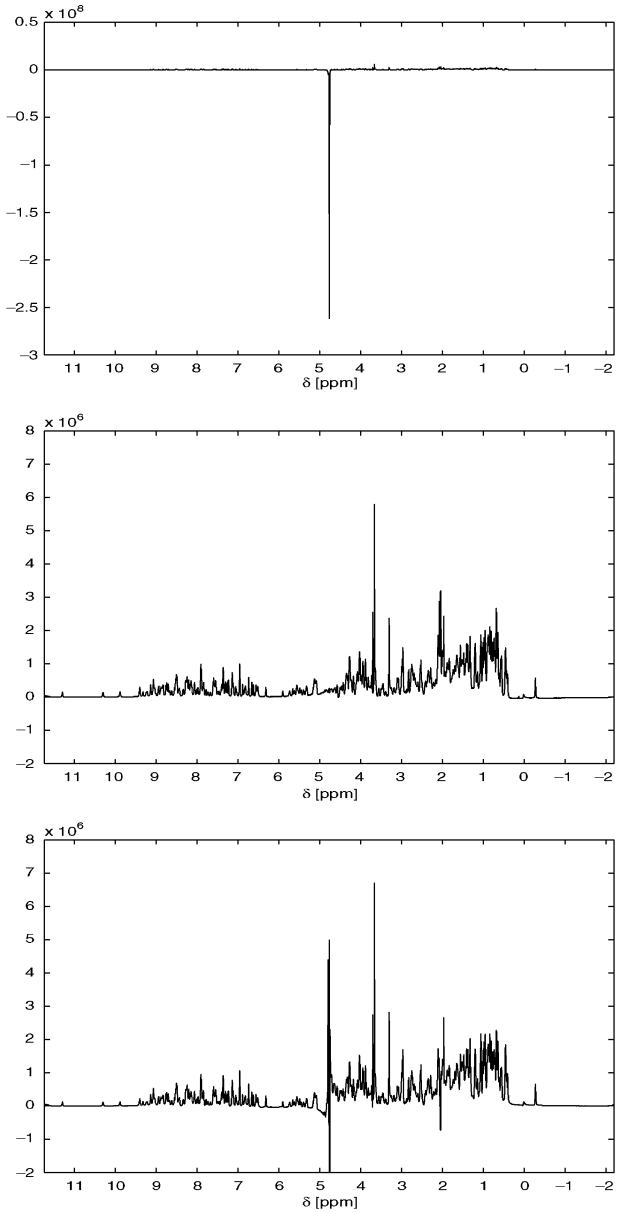

Fig. 6. HPr: *top*: one-dimensional slice of the original 2-D NOESY spectrum corresponding to the shortest evolution period t_1, *middle*: corresponding protein spectrum obtained by subtracting the local PCA approximation to the water artefact FID from the total FID, *bottom*: corresponding protein spectrum reconstructed with the dAMUSE and BSS-AutoAssign algorithms.

2) The Protein HPr: As another example the 2-D NOESY NMR spectra of the *Histidine containing phospho-carrier protein* HPr of the bacterium *Staphylococcus carnosus* with 88 amino acids have been analyzed. The NMR sample studied contained 4.3 mM HPr in $90\%\mathrm{H_2O}/10\%\mathrm{D_2O}$ and the pH was adjusted to 7.2. The spectrum using a mixing time of 150 ms was acquired at a proton resonance frequency of 800.13 MHz with 1024×8192 time domain data points in t_1 and t_2 directions, respectively. Phase-sensitive detection in the t_1 direction was obtained using time-proportional phase increments (TPPI). A relaxation delay of 2.37 s between the scans was applied. The spectrum was measured at 298 K. In this case, 1024 evolution periods t_1 have been used, hence, a data matrix $\mathbf{X}$ of dimension 256×2048 resulted. The spectrum shown in Fig. 6(a), representing a 1-D slice corresponding to the shortest evolution period, presents an example with an especially huge, weakly presaturated water resonance. Fig. 6(b) shows the *approximated* spectrum obtained after approximating the contribution of the *water* protons to the observed FID with local PCA as described above. As the water contribution was exceptionally dominant in this case, the local PCA approximation yielded a very good estimate of the water FID, hence, a practically artifact-free protein spectrum resulted. Again note, that this must not necessarily hold for other evolution periods as well. But this is of no importance as the local PCA approximation of the water FID is only needed to yield a good reference in the cost function of the SA algorithm where the estimated uncorrelated components are assigned to the water or the protein. Fig. 6(c) shows the *reconstructed* spectrum obtained using the algorithm dAMUSE together with the algorithm BSS-AutoAssign. Note that the GEVD-MP algorithm removed the water artifact almost completely [23] but it also lead to distortions of nearby protein peaks and furthermore resulted in intensity changes of protein peaks farther away from the water resonance. After all the SNR ratio was far less than with the reconstructed spectrum obtained with the algorithm dAMUSE. The latter spectrum also shows no distortions of protein peaks but, as a little grain of salt, contains a delta-like spike stemming from the water artifact. The small remnants of the water artifact can only be removed at the expense of disturbing the intensities of some protein peaks as the decomposition of the original signals in uncorrelated components is not perfect, of course. So in all cases our foremost interest was to leave all protein resonances unchanged in their intensities.

IV. Conclusion

The separation of artifacts from biomedical signal recordings is one of the more prominent applications of blind source separation techniques. The assignment of the artifact-related uncorrelated components estimated is, however, not a trivial task and often done by hand. In this paper, we presented an automatic assignment tool of uncorrelated components, called BSS-AutoAssign, which uses local PCA to approximate the prominent water artifact in 2-D NOESY protein NMR spectra and defines a suitable cost function to be optimized by SA.

Local PCA tries to approximate the water related component to the measured FID which then can be subtracted from the total FID observed. This is done only for the FIDs corresponding to the shortest evolution period where the contribution of the water artifact is most prominent. This approximation is then used within a SA procedure to assign those estimated ICs which most closely resemble the approximated water FID from the local PCA approximation. It is then assumed that this assignment of the estimated ICs also holds with all other evolution periods where no local PCA approximations have been determined. Doing so would result in a computational effort which seems prohibitive. The FID resulting from the local PCA approximation can be Fourier transformed to yield an almost artifact-free protein spectrum. The results obtained look very convincing from a visual inspection of the spectra. However, they remove any signal in the spectral region of the water peak. Hence, all information about protein peaks in that area is inevitably lost (see Fig. 7).

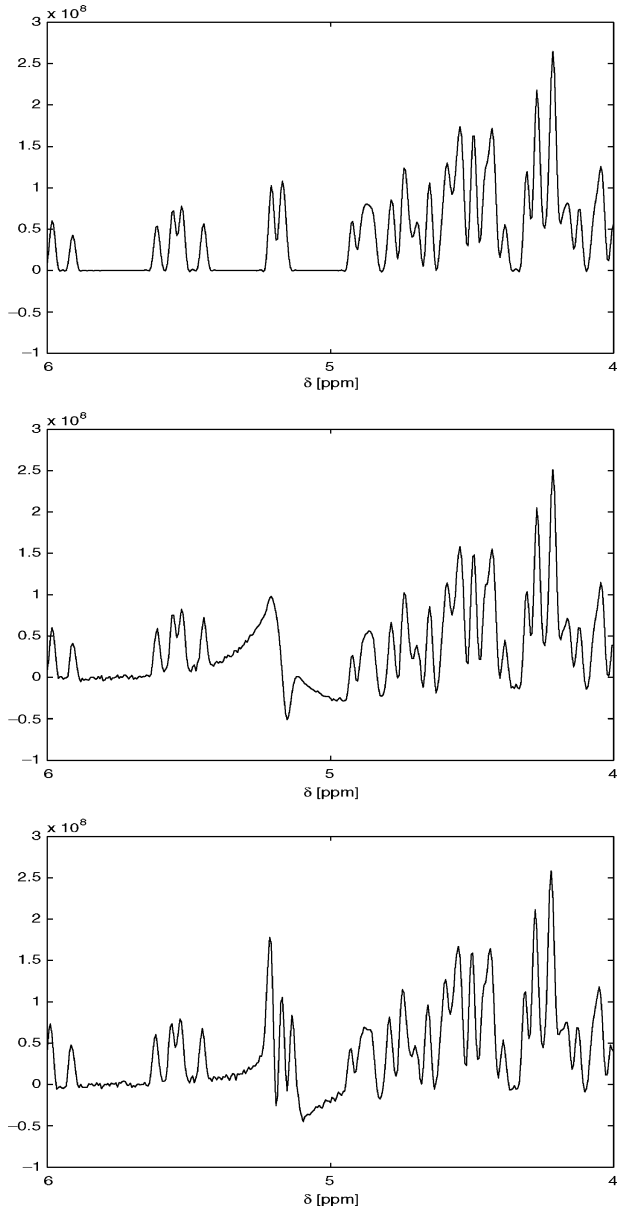

Fig. 7. Theoretical protein spectrum: *top*: expanded region of the original spectrum corresponding to Fig. 1, *middle*: expanded region of the approximated spectrum corresponding to Fig. 3, *bottom*: expanded region of the theoretical spectrum reconstructed with dAMUSE and BSS-AutoAssign corresponding to Fig. (3).

A much more versatile analysis method is based on the recently proposed algorithm dAMUSE in combination with BSS-AutoAssign. A close inspection of the results obtained with the theoretical spectra of *Tm*CSP demonstrate convincingly that BSS-AutoAssign in combination with dAMUSE retains information about spectral features in the region of the water artifact where the local PCA approximation and all other known water suppression techniques erase all spectral features whatsoever (see Fig. 7). This demonstrates that with the method described here it is possible to obtain additional structurally relevant restraints from the experimental NOESY spectra which will enter the structure calculation process. Since the quality of the obtained 3-D structures correlates with the completeness of the correctly identified restraints [29], this will lead to an improvement of the resulting structures. Completeness is hereby defined as the ratio of the number of matched observed NOEs to the number of expected NOEs. Furthermore, baseline artifacts are cured with dAMUSE and BSS-AutoAssign in all cases allowing for a better determination of peak integrals entering any structure determination calculation, which will also increase the quality of the resulting protein structures by allowing the use of smaller error bounds for the corresponding distance restraints [30]. With the local PCA approximation alone, often severe baseline distortions remain which hampers the subsequent structure determination considerably. Hence, a more robust method is needed to reliably extract the water artifacts. The algorithms dAMUSE in combination with BSS-AutoAssign provide such a method and seem a promising tool for an automatic assignment and removal of artifacts in biomedical signal recordings. Further investigations concerning other biomedical signals are under way in our laboratories.

REFERENCES

[1] K. H. Hausser and H. R. Kalbitzer, NMR Med. Biol. 1989.
[2] M. Adler and G. Wagner, "Removal of dispersive baseline distortions caused by strong water signals," *J. Magn. Reson.*, vol. 91, pp. 450–454, 1991.
[3] M. Friedrichs, W. Metzler, and L. Mueller, "Removal of diagonal peaks in two-dimensional NMR spectra by means of digital filtering," *J. Magn. Reson.*, vol. 95, pp. 178–183, 1991.
[4] D. Marion, M. Ikura, and A. Bax, "Improved solvent supression in one- and two-dimensional NMR spectra by convolution of time-domain data," *J. Magn. Reson.*, vol. 84, pp. 425–430, 1989.
[5] P. Tsang, P. Wright, and M. Rance, "Signal supression in the frequency domain to remove undesirable resonances with dispersive lineshapes," *J. Magn. Reson.*, vol. 80, pp. 210–215, 1990.
[6] Y. Kuroda, A. Wada, T. Yamazaki, and K. Nagayama, "Postacquisition data processing method for suppression of the solvent signal," *J. Magn. Reson.*, vol. 84, pp. 604–610, 1989.
[7] L. Mitschang, C. Cieslar, T. Holak, and H. Oschkinat, "Application of the karhunen-loeve transformation to the suppression of undesired resonances in three-dimensional NMR," *J. Magn. Reson.*, vol. 92, pp. 208–217, 1991.
[8] J. Hardy and P. Rinaldi, "Principal component analysis for artifact reduction in COSY spectra," *J. Magn. Reson.*, vol. 88, pp. 320–333, 2003.
[9] D. Brown and T. Campbell, "Enhancement of 2D NMR spectra using singular value decomposition," *J. Magn. Reson.*, vol. 89, pp. 255–264, 1990.
[10] D. Barache, J.-P. Antoine, and J.-M. Dereppe, "The continous wavelet transform, an analysis tool for NMR spectroscopy," *J. Magn. Reson.*, vol. 128, pp. 1–11, 1997.
[11] J.-P. Antoine, A. Coron, and J.-M. Dereppe, "Water peak suppression: time-frequency vs time-scale approach," *J. Magn. Reson.*, vol. 144, pp. 189–194, 2000.
[12] U. Günther, C. Ludwig, and H. Rüterjans, "WAVEWAT-improved solvent suppression in NMR spectra employing wavelet transforms," *J. Magn. Reson.*, vol. 156, pp. 19–25, 2002.
[13] A. M. Tomé, "An iterative eigendecomposition approach to blind source separation," in *Proc. 3rd Intern. Conf. on Independent Component Analysis and Signal Separation, ICA'2003*, San Diego, CA, 2001, pp. 424–428.
[14] K. Stadlthanner, F. Theis, E. W. Lang, A. M. Tomé, W. Gronwald, and H. R. Kalbitzer, "A matrix pencil approach to the blind source separation of artifacts in 2D NMR spectra," *Neural Inf. Process.—Lett. Rev.*, vol. 1, pp. 103–110, 2003.
[15] K. Stadlthanner, A. M. Tomé, F. J. Theis, W. Gronwald, H. R. Kalbitzer, and E. W. Lang, "On the use of independent component analysis to remove water artifacts of 2D NMR protein spectra," presented at the 7th Portuguese Conf. Biomedical Engineering, BIOENG'2003, Lisbon, Portugal, 2003.
[16] S. Kirkpatrick, C. D. G. , Jr., and M. P. Vecchi, "Optimization by simulated annealing," *Science*, vol. 220, p. 671, 1983.

[17] A. M. Tomé, A. R. Teixeira, E. W. Lang, K. Stadlthanner, A. Rocha, and R. Almeida, "dAMUSE a new tool for denoising and blind source separation," *Digital Signal Process.*, vol. 15, pp. 400–421, 2005.
[18] T. Schreiber and H. Kantz, "Nonlinear projective filtering II: Application to real time series," presented at the NOLTA, Crans Montana, Switzerland, 1998.
[19] T. Schreiber and H. Kantz, "Nonlinear projective filtering II: Application to real time series," in *Proc. Nolta*, 1998.
[20] M. Ghil, M. Allen, M. D. Dettinger, and K. Ide, "Advanced spectral methods for climatic time series," *Rev. Geophys.*, vol. 40, no. 1, pp. 3.1–3.41, 2002.
[21] L. Tong, R.-w. Liu, V. C. Soon, and Y.-F. Huang, "Indeterminacy and identifiability of blind identification," *IEEE Trans. Circuits Syst.*, vol. 38, no. 5, pp. 499–509, May 1991.
[22] A. M. Tomé, A. R. Teixeira, E. W. Lang, K. Stadlthanner, and A. Rocha, "Blind source separation using time-delayed signals," in *Proc. Int. Joint Conf. Neural Networks, IJCNN'2004*, Budapest, Hungary, 2004, vol. CD.
[23] K. Stadlthanner, A. M. Tomé, F. J. Theis, W. Gronwald, H. R. Kalbitzer, and E. W. Lang, "Blind source separation of water artifacts in NMR spectra using a matrix pencil," in *Proc. 4th Int. Symp. Independent Component Analysis and Blind Source Separation, ICA'2003*, Nara, Japan, 2003, pp. 167–172.
[24] K. Stadlthanner, A. M. Tomé, F. J. Theis, E. W. Lang, W. Gronwald, and H. R. Kalbitzer, "Separation of water artifacts in 2D NOESY protein spectra using congruent matrix pencils," *Neurocomputing*, 2005, accepted.
[25] A. R. Teixeira, A. M. Tomé, E. W. Lang, and K. Stadlthanner, "Delayed AMUSE—A tool for blind source separation and denoising," in *Lecture Notes in Computer Science*. Berlin, Germany: Springer-Verlag, vol. 195, Independent Component Analysis and Blind Signal Separation, Proc. ICA'2004, pp. 287–294.
[26] V. Moskvina and K. M. Schmidt, "Approximate projectors in singular spectrum analysis," *SIAM J. Mater. Anal. Applicat.*, vol. 24, no. 4, pp. 932–942, 2003.
[27] L. Parra and P. Sajda, "Blind source separation vis generalized eigenvalue decomposition," *J. Mach. Learn. Res.*, vol. 4, pp. 1261–1269, 2003.
[28] A. Görler and H. R. Kalbitzer, "RELAX, a flexible program for the back calculation of NOESY spectra based on a complete relaxation matrix formalism," *J. Magn. Reson.*, vol. 124, pp. 177–188, 1997.
[29] W. Kremer, B. Schuler, S. Harrieder, M. Geyer, W. Gronwald, C. Welker, R. Jänicke, and H. R. Kalbitzer, "Solution NMR structure of the coldshock protein from the hyperthermophilic bacterium thermotoga maritima," *Eur. J. Biochem.*, vol. 268, pp. 2527–2539, 2001.
[30] J. Doreleijers, M. Raves, T. Rullmann, and R. Kaptein, "Completeness of NOE's in protein structures: a statistical analysis of NMR data," *J. Biomolecular NMR*, vol. 14, pp. 123–132, 1999.
[31] J. Evans, *Biomolecular NMR Spectroscopy*. Oxford, U.K.: Oxford Univ. Press, 1995.

M. Böhm received the physics diploma from the University of Regensburg. Regensburg. Germany, in 2004. He is currently a doctoral student at the Institute of Biophysics, Neuro- and Bioinformatics Group, University of Regensburg.

His scientific interests are in the fields of blind source separation, bio-inspired optimization and brain modeling.

K. Stadlthanner received the physics diploma from the University of Regensburg, Regensburg, Germany, in 2003. He is currently a doctoral student at the Institute of Biophysics, Neuro- and Bioinformatics Group, University of Regensburg.

His scientific interests are in the fields of biological data processing and analysis by means of blind source separation and support vector machines.

P. Gruber received the mathematics diploma from the University of Regensburg, Regensburg, Germany, in 2002. He is currently a doctoral student at the Institute of Biophysics, Neuro- and Bioinformatics Group, University of Regensburg.

His scientific interests are in the fields of statistical signal processing and machine learning.

F. J. Theis (M'05) received the Ph.D. degree in physics from the University of Regensburg, Regensburg, Germany, and the Ph.D. degree in computer science from the University of Granada, Granada, Spain.

Currently, he works as Postdoctoral Researcher at the Neuro- and Bioinformatics group of the University of Regensburg. His research interests include statistical signal processing, linear and nonlinear ICA, and overcomplete blind source separation based on sparse component analysis.

E. W. Lang received the physics diploma in 1977, the Ph.D. degree in physics in 1980, and habilitated in biophysics in 1988 from the University of Regensburg, Regensburg, Germany.

He is Adjunct Professor of biophysics at the University of Regensburg, where he is heading the Neuro- and Bioinformatics Group. Currently, he serves as Associate Editor of *Neurocomputing* and *Neural Information Processing-Letters and Reviews*. His current research interests include biomedical signal and image processing, independent component analysis and blind source separation, neural networks for classification and pattern recognition, and stochastic process limits in queuing applications.

A. M. Tomé (S'86–M'90) received the Ph.D. degree in electrical engineering from University of Aveiro, Aveiro, Portugal, in 1990.

Currently, she is Associate Professor of Electrical Engineering with the Department of Electronics and Telecomunications/IEETA of the University of Aveiro. Her research interests include digital and statistical signal processing, independent component analysis, and blind source separation, as well as classification and pattern recognition applications.

A. R. Teixeira received the diploma degree in mathematics applied to technology from University of Porto, Porto, Portugal, in 2003. She is currently working towards the M.Sc. degree in electronics and telecommunications at the University of Aveiro, Aveiro, Portugal.

Her research interests include biomedical digital signal processing and principal and independent component analysis.

W. Gronwald graduated from the University of Braunschweig, Braunschweig, Germany, in 1991.

He is currently a Lecturer in Biophysics at the University of Regensburg, Regensburg, Germany. His research interests include development and application of computational methods for three-dimensional protein structure determination. (Home page: http://www-nw.uni- regensburg.de/grw28475.biophysik.biologie.uni-regensburg.de/).

H. R. Kalbitzer received the M.D. degree in physics and medicine from the University of Heidelberg, Heidelberg, Germany, in 1976 and 1981, respectively.

He is currently Professor of Biophysics at the University of Regensburg, Regensburg, Germany. His research interests include structural biology, NMR spectroscopy, and software development. (Home page:http://biologie.uni-regensburg.de/Biophysik/Kalbitzer).